https://doi.org/10.37434/tpwj2022.02.04

# DESTRUCTION OF WELDED JOINTS OF SINGLE-CRYSTAL HIGH-TEMPERATURE NICKEL ALLOYS AT TENSILE TESTING

**K.A. Yushchenko, B.O. Zaderii, I.S. Gakh, G.V. Zviagintseva, T.O. Aleksiienko**

E.O. Paton Electric Welding Institute of the NASU
11 Kazymyr Malevych Str., 03150, Kyiv, Ukraine

**ABSTRACT**

Mechanical properties were determined and features of destruction of welded joints on single-crystals of high-temperature nickel alloys at tensile testing in the range of temperatures close to working temperatures were studied. Two characteristic temperature ranges of destruction were found: 500–800, 800–1200 °C. In the first temperature range welded sample destruction occurs in the base metal at mixed fracture mode: brittle, quasibrittle and ductile. In the second range destruction takes place in the weld metal, fracture is multicenter, predominantly brittle with presence of secondary cracks. The considered features are related, mainly, to changes of the initial structure of the single-crystal, as a result of solidification and at cooling of the weld metal. These mainly are formation of a multilevel substructure, refinement of dendrites, γ- and γ′-phases, eutectic formations and carbides at reduction of dendrite liquation of the weld metal.

**KEY WORDS:** single-crystal, high-temperature nickel alloys, welded joint, weld, tensile testing, temperature ranges of destruction, destruction features, microstructure

## INTRODUCTION

Improvement of the effectiveness of modern gas turbine engines (GTE) is achieved due to increase of gas temperature at the turbine inlet, which, in its turn, makes certain requirements on the high-temperature strength of materials used to manufacture the components and parts of the hot path [1–3]. Satisfying these requirements through application of high-temperature nickel alloys (HTNA) and multicomponent alloying, optimization of the structure, in particular, single-crystal one, has practically exhausted its potential. Solving this problem due to a change and optimization of the geometry of individual parts often becomes a complex technology and cost problem. This is particularly evident, when growing one of the critical and complex-loaded GTE parts — a single-crystal blade with transpiration and other cooling methods. Here, alongside producing a perfect single-crystal structure of a certain crystallographic orientation, it is necessary to ensure a complex geometry of both the blade outer surface, and inner cooling channels of a certain cross-section and surface finish [3, 4].

Despite the advances of the technology of growing single-crystals by directional solidification method, manufacturing welded parts, made up of individual, more readily adaptable-to-fabrication structural elements, is ever wider used [5–10].

A sufficiently large number of publications are devoted to the subject of both welding and growing HTNA single-crystals. However, there is practically no information about the mechanical properties and destruction features of either welded joints as a whole, or of the welds taken separately.

The objective of this work was studying the properties and destruction features of welded joints of HTNA single-crystals at elevated temperatures, taking into account the need to develop a technology for structure welding.

## INVESTIGATION PROCEDURES

HTNA widely applied in industry — ZhS26 was selected as the initial material for work performance. The alloy chemical composition is as follows, wt.%: 4.3–5.6 Cr, 4.5–8.0 Al, 0.8–1.2 Ti, 0.8–1.4 Mo; 10.9–12.5 W, 8.0–10.0 Co, 1.4–1.8 Nb, 0.22–0.27 Mn, 0.9–1.1 Fe, 0.8–1.2 V, 0.13–0.18 C. Welding of 1.5–2.5 mm samples, cut out of blanks, produced by the method of directional high-gradient solidification, was performed by the electron beam, as the most precise and widely accepted method in aircraft construction. The modes and crystallographic orientation of the samples were selected proceeding from the condition of sound formation of the welds, preservation of the initial crystallographic orientation (not more that 10° deviation was allowed), ensuring perfection of the single-crystal structure (absence of high-angle grain boundaries) of the weld metal [7, 11–13]. Samples for welding, testing and investigations were cut out by spark method with subsequent grinding. The cross-section and length of the working part of tensile samples were equal to ~4 mm$^2$ and 18 mm, respectively.

Mechanical testing was conducted in ALLO-TOO unit of Gleeble type in a chamber with residual pressure of $<10^{-2}$ Pa at load rate of $1.84 \cdot 10^{-3}$ s$^{-1}$. The range of testing temperatures was equal to 500–1200 °C,

which corresponded to average operating parameters of GTE blades from ZhS26 alloy. Temperature monitoring, load recording and graphic presentation of the "load-displacement" dependencies were performed using software [14].

Tested were samples of two types: with longitudinal and transverse location of the weld relative to the load direction (Figure 1). As the cross-section of the weld and that of the sample with its longitudinal location (Figure 1, *b*) coincide, their testing allows evaluation of the influence of structural changes resulting from electron beam remelting and solidification at single-crystal welding. Testing samples with a transverse weld location gives an idea about the behaviour of the welded joint as a whole during testing, which consists of a combination of different structural regions: base metal, HAZ, and weld metal.

Crystallographic orientation of the initial samples, welded joints and structural elements was assessed involving the procedure of X-ray diffractometry by analysis of the distribution of intensity of reflections on the pole figures, θ–2θ X-ray patterns ($Iq_{\parallel}$) and in the plane, normal to the diffraction vector $q$–$Iq_{\perp}$ [15–17]. Structural state of welded joints and fracture pattern were studied by the methods of optical microscopy ("MIM-7", "Neophot-32"), electron scanning microscopy (Camscan-4, SEM-515 PHILIPS), distribution of chemical elements in individual components of the fracture and structure was investigated by EDX analysis in JEOL microscope with JNCO attachment.

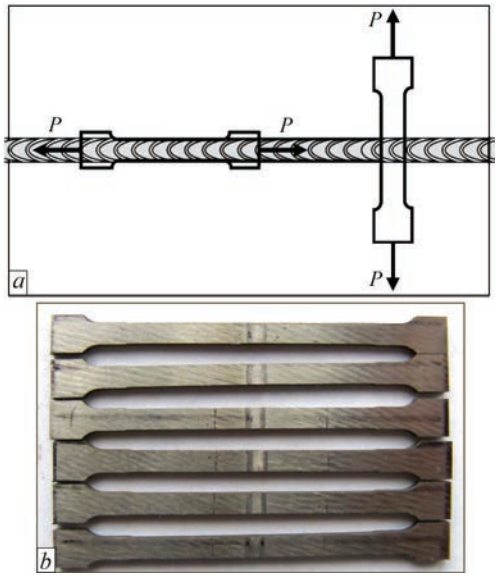


**Figure 1.** Scheme of cutting out tensile samples from welded joints of HTNA single-crystals and orientation of load *P* at testing (*a*) and general view of tensile samples (*b*)

## RESULTS AND DISCUSSION

### *WELDED JOINT STRUCTURE*

The welded alloy (base metal) in the initial condition is characterized by a developed cell-dendrite structure, which includes a finely-dispersed strengthening γ′-phase ($Ni_3Al$), uniformly distributed in γ-solid solution of the nickel matrix (Figure 2, *a*) with individual inclusions of γ–γ′ eutectic formations and carbide precipitates of a complex composition and topography. Eutectic formations and carbides are predominantly

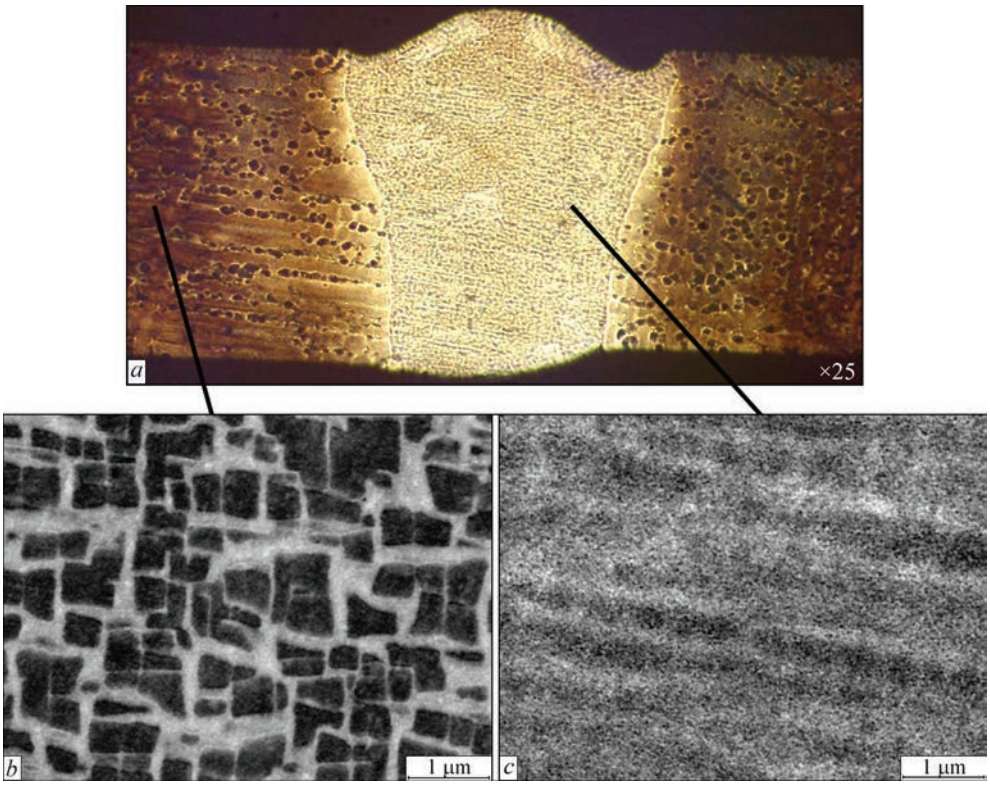


**Figure 2.** Macrostructure of welded joint (*a*), microstructure (γ/γ′) of initial metal (*b*) and weld (*c*) of HTNA single-crystal

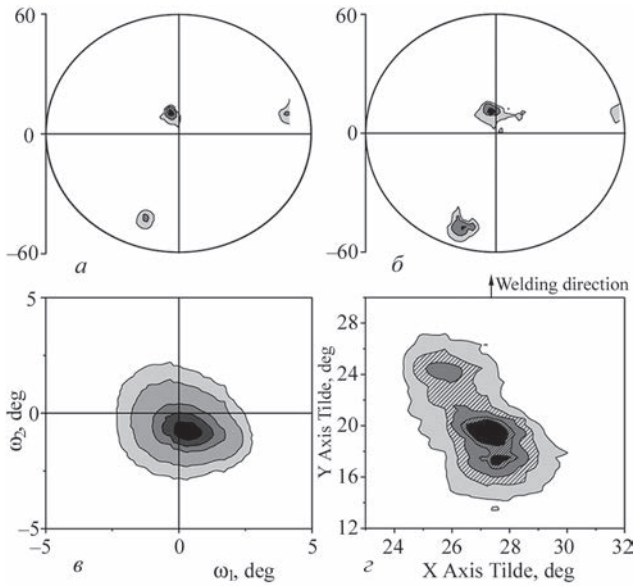


**Figure 3.** Pole figures {220} (*a*, *b*) and typical 2D distribution of $Iq_{\perp}$ of {220} reflections (*c*, *d*) in the initial growth HTNA single-crystal (*a*, *c*) and in the weld (*b*, *d*), *x*, *y* — angular instrumental coordinates; $\omega_1$ and $\omega_2$ — angular coordinate of reciprocal space

located in the interdendritic, interphase gaps. γ′-phase content in the alloy is equal to ~61 %.

Welded joint structure differs from that of the base metal by noticeably smaller dimensions of the structural components. Thus, if the interdendritic spacing (λ) of the base metal is equal to 200–300 μm, in the weld it decreases to 30–50 μm on the weld axis and to 3–12 μm near the fusion line (Figure 2, *b*). The size of γ′-phase particles ($d\gamma_1$) in the initial metal is 0.3–0.6 μm, in the weld it is by an order of magnitude smaller — 0.04–0.08 μm, and in the HAZ it is 0.3–0.02 μm. In connection with reduction of the dimensions of the structural components the chemical heterogeneity of the weld metal markedly decreases (Table 1).

The selected modes and welding scheme allowed limiting the deviation of crystallographic orientation of the welded joint from the initial value by not more than 7° (Figure 3). The disorientation of the weld metal structure as a result of the influence of the thermodeformational cycle of welding can be more clearly assessed by $Iq_{\perp}$ distribution (Figure 3). Distribution of $Iq_{\perp}$ and its fragmentation according to [15–19] corresponds to formation of a substructure with a multilevel directional disorientation of the metal by the dislocation boundaries that does not exceed 2°. Formation of a multilevel structure leads to the conclusion about the existence of residual stresses in the weld. The found shifting of the peak of $Iq_{\parallel}$ distribution in "θ–2θ" X-ray patterns (Figure 4)* towards the smaller angle of 2θ reflection points to the presence of tensile stresses in the direction along the weld [15–17]. Calculation, made using the Hooke's law and allowing for shifting of $Iq_{\parallel}$ peak showed that for welds of (110) orientation can reach 397 MPa, and for (111) it is 520 MPa.

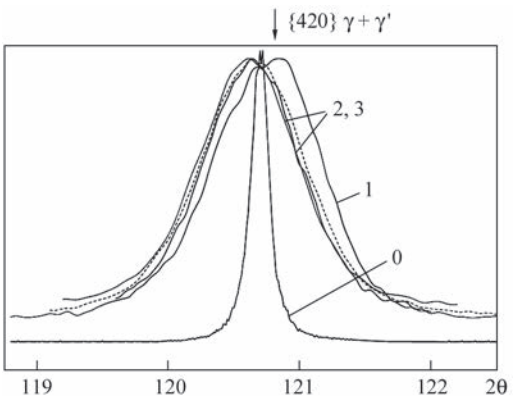


**Figure 4.** "θ–2θ" distribution of $Iq_{\parallel}$ of {420} reflections in the standard (0), in the initial metal (*1*) and along the axis of weld metal (*2*, *3*) of single-crystal ZhS26

*DESTRUCTION FEATURES OF SAMPLES WITH TRANSVERSE LOCATION OF WELDS (WELDED JOINTS)*

In the generalized form, the results of rupture testing of the welded samples are given in Figure 5 as $\sigma_t$ and $\sigma_{0.2}$ dependencies on temperature. They can be conditionally subdivided into two regions. The first region (testing temperature $T_{test} \le 800$ °C) is characterized by a smaller dependence of $\sigma_t$ and $\sigma_{0.2}$ on temperature, more noticeable influence of the crystallographic orientation and sample fracture in the base metal. In the second region ($T_{test} > 800$ °C) an intensive lowering of $\sigma_t$ and $\sigma_{0.2}$ values, leveling of the influence of the initial crystallographic orientation are observed, and sample fails through the weld.

The above-mentioned fracture features of the welded joints can be explained as follows. Welded joints are a composite material, which consists of regions of different structure: base metal, HAZ and weld. Owing to more than an order higher dispersity of the structural components, according to Hall–Patch

**Table 1.** Dendritic liquation $k_l = C_d/C_{int.sp}$ of the main chemical components of initial ZhS26 alloy and weld metal ($k_l$ — liquation coefficient, $C_d$ — concentration on dendrite axis, $C_{int.sp}$ — concentration in interdendritic space)

| Region | Al | Ti | V | Cr | Co | Nb | Mo | W |
|---|---|---|---|---|---|---|---|---|
| Initial metal | 0.7 | 0.55 | 1.28 | 1.98 | 1.2 | 0.6 | 1.6 | 1.89 |
| Weld metal | 0.94 | 0.7 | 1.2 | 1.04 | 1.02 | 0.9 | 1.08 | 1.24 |

*O.P. Karasevska took part in word performance.

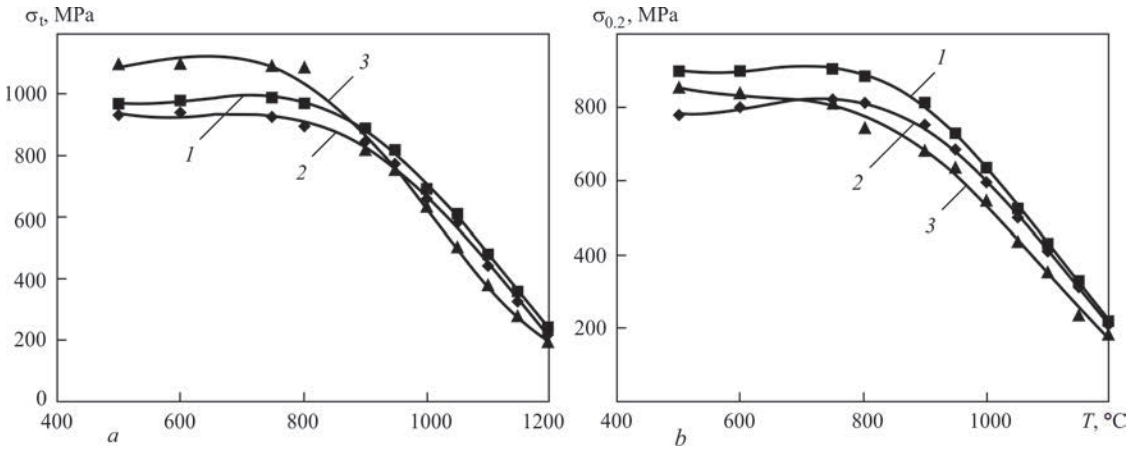


**Figure 5.** Dependence of ultimate strength $\sigma_t$ (*a*) and yield limit $\sigma_{0.2}$ (*b*) on testing temperature of welded samples of ZhS26 alloy single-crystals in the transverse (*1*, *2*) and longitudinal (*3*) position of the welds. Load orientation: ~<100> (*1*, *3*) and ~<110> (*2*)

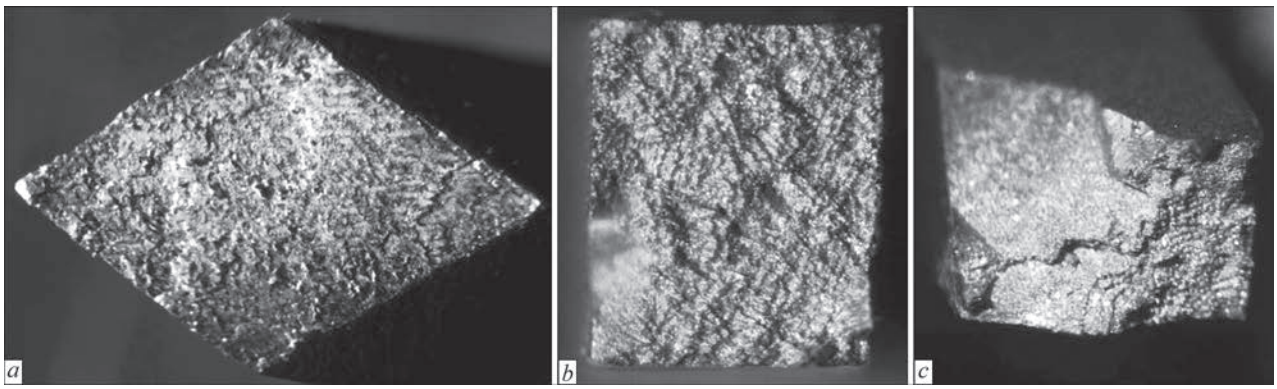


**Figure 6.** Appearance of fractures in welded joint of ZhS26 alloy single-crystal of orientation close to [011], after testing for uniaxial tension at the temperature of: *a* — 600 °C; *b* — 1050; *c* — 900

law [19–21], the weld metal is in a more strengthened state. Strengthening is also related to the observed increase of the density of unpinned chaotic dislocations in the weld metal (see Figure 4).

At increase of testing temperature to 800 °C and higher, fracture shifts into the HAZ and the weld, as a result of weakening of the strengthening effect of the finely-dispersed structure, as well as a result of increase of defect mobility [21, 22] on the low-angle boundaries of the weld metal.

Fractures of samples tested at moderate (≤600 °C) temperatures, are characterized by quasicleavage topography, combined with presence of regions of fine-cellular tear with weakly manifested elongation (Figures 6, 7). At increase of test temperature to 800 °C, the fractures develop a mixed fracture mode — a combination of brittle (30–35 %), quasibrittle (20–25 %) and ductile variants (45–50 %). Accordingly, the fracture surface microrelief is represented by sites of low-ductility shear in metal and quasicleavage facets of 50–60 μm size, steps of 1–20×20–100 μm of brittle banded appearance, and shallow dispersed pits (0.5–1.5 μm) of ductile fracture (Figure 7). As the temperature approaches 800 °C, the ductile fracture fraction rises up to 50–60 %, fracture takes the pit-ductile form, and brittle fracture elements are gradually replaced by relief pits, fringed by tear ridges. Investigations of the side surfaces of

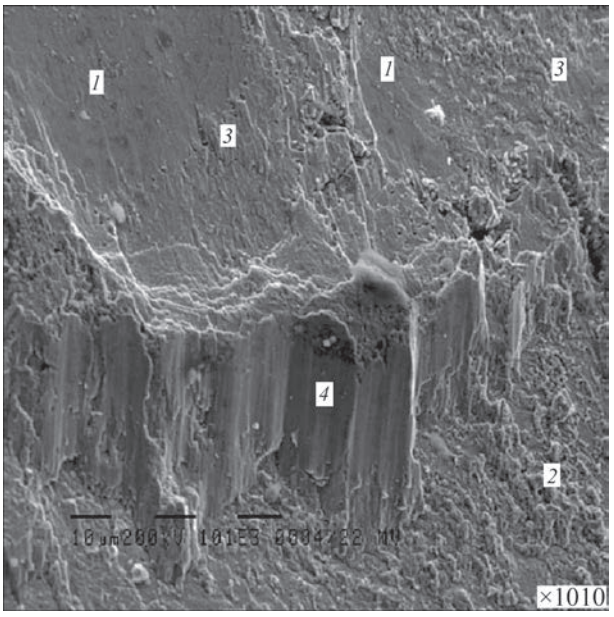


**Figure 7.** Fragment of fracture surface of the welded joint. Testing temperature of 600 °C (*1* — steps with brittle banded relief; *2* — dispersed pits of ductile fracture; *3* — shear facets, quasibrittle failure areas; *4* — banded relief, brittle fracture mode, band width $\Delta_b$ = 10 – 20 μm)

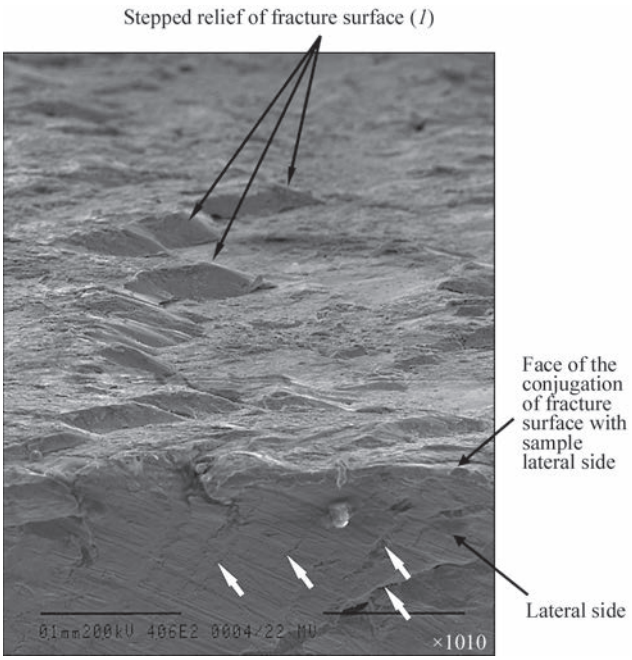


**Figure 8.** Conjugation of the sample lateral side and fracture surface. Light arrows mark the microcracks on the sample side surface, formed by plastic shear mechanism along the easy slip planes {111} <110>. Test temperature of 600 °C (*1* — steps with brittle banded relief)

samples, broken in this temperature range (Figure 8), revealed the presence of slip bands, relief shear areas and microcracks which pass at a small angle to fracture plane, which illustrates the shear mode of fracture along the most loaded slip systems [18, 19, 23].

Welded joint fracture in the temperature range of 900–1200 °C runs in the weld, and is characterized by multicellularity (Figure 9). The fractures are represented by such elements as: cleavage facets — of ~10–20 μm size and quasicleavage facets of ~8–15 μm, carbide type phase precipitates (0.3–0.4×3.0–7.0 μm) on cleavage facets, secondary microcracks (20–100 μm) and coarse delaminations (100–350 μm). Individual local areas of the ductile component (5–7 %) allow us assuming that fracture runs with a certain fraction of plastic deformation. The general fracture mode is brittle (~90–93 %).

### *DESTRUCTION FEATURES OF SAMPLES WITH A LONGITUDINAL LOCATION OF WELDS*

At testing with longitudinal loading in the temperature range of 500–600 °C, the destruction of the welds occurs in the ductile mode with pit size of ~2–9 μm in the fracture (Figure 10). At increase of testing temperature up to 800 °C the failure mode changes to a mixed one, areas of quasibrittle failure of ~3.0–9.5 μm are observed in the fracture near the pits. At further increase of temperature up to 1200 °C, the mixed failure is characterized by increase of the fraction of quasibrittle component, secondary cracks

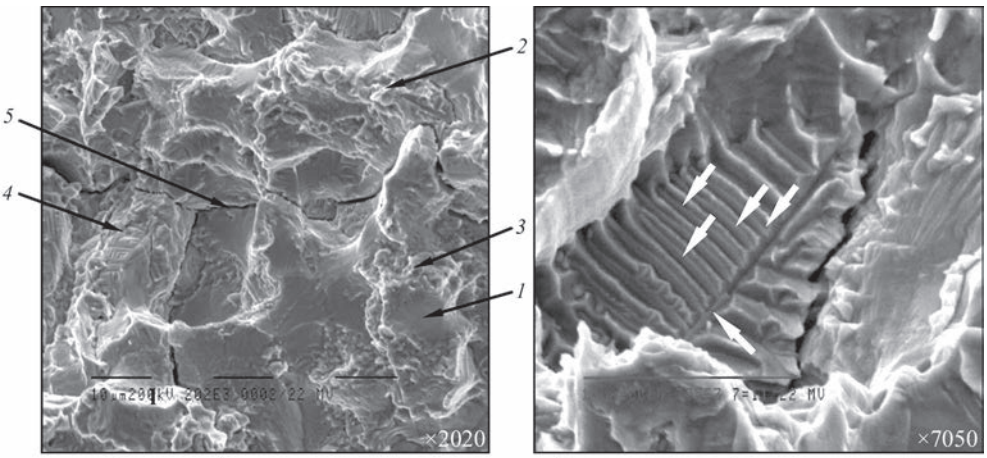


| Elements | 1 Brittle | 2 Quasibrittle | 3 Ductile | 4 PP |
|---|---|---|---|---|
| Al | 2.64 | 2.86 | 1.92 | 3.01 |
| Ti | 1.66 | 1.22 | 1.58 | 3.77 |
| V | 0.35 | 0.34 | 0.41 | 0.45 |
| Cr | 4.45 | 5.63 | 5.75 | 4.7 |
| Co | 9.31 | 9.47 | 9.61 | 6.92 |
| Ni | 69.86 | 62.72 | 68.58 | 50.75 |
| Nb | 1.47 | 1.78 | 1.75 | 12.05 |
| Mo | 1.67 | 2.66 | 2.06 | 5.3 |
| W | 8.6 | 13.32 | 8.35 | 13.05 |

**Figure 9.** Fragments of fracture surface in different regions of weld metal at welded joint testing for uniaxial tension and chemical element content in the fracture (wt.%). Testing temperature was 1050 °C. Welded joint orientation was [100]. *1* — brittle fracture: size of cleavage facets $d_f$ = 10–20 μm; *2* — quasibrittle fracture; *3* — local regions of ductile fracture: dispersed pits of size $d_p$ = 1–2 μm; *4* — phase precipitates (PP); *5* — secondary cracks $l_{cr}$ ~ 20–100 μm (light arrows — PP)

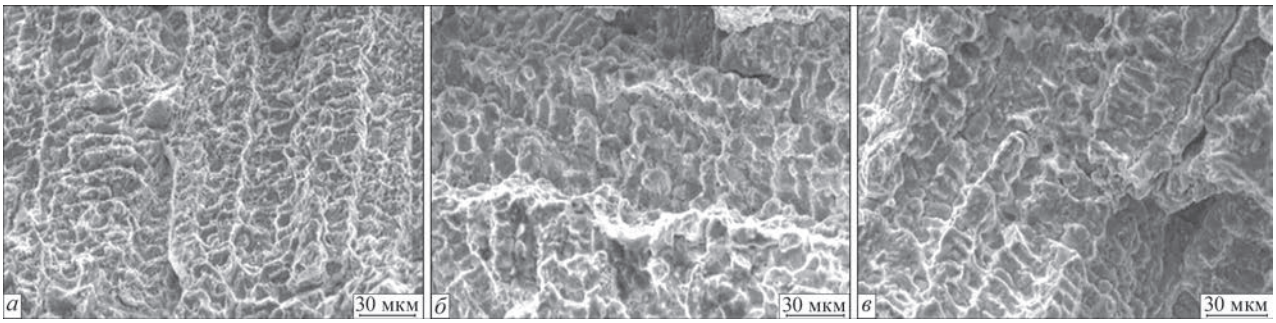


**Figure 10.** Fragments of fracture surface of a weld of ZhS26 alloy single-crystal. Testing for uniaxial tension in the longitudinal direction at temperatures of: 600 °C (*a*), 1050 (*b*), 1200 (*c*)

are observed (Figure 10), and the size of failure elements on the fracture surface is equal to 3.5–10.0 μm (1050 °C) and 4.5–10.5 μm (1200 °C). The fractures inherit the dendrite morphology of the microstructure of the weld, and of structural formation defects, developing during solidification.

A certain difference in fracture morphology, as in the properties of welds, tested in the longitudinal and transverse directions, is most probably, associated with different orientation of the weld metal dendritic structure relative to the direction of the applied load.

Note the complexity and multifaceted nature of the fractures, nonuniformity of the relief that reflects the heterogeneity of the structure and crystallographic orientation of individual regions of the welded joints.

Proceeding from analysis of the results of the above studies, features of destruction, mechanical properties and structure, we can conclude that the established difference in the properties and characteristic deformations and failure of welded joints of ZhS26 single-crystals in the high- and low-temperature range is largely determined by the nature of structural changes, occurring as a result of welding.

## CONCLUSIONS

1. When assessing the destruction features and properties of nickel alloy welded joints, they should be regarded as a composite material, consisting of areas of different structure.

2. As a result of welded joint testing for uniaxial tension in the temperature range of 500–1200 °C, two destruction regions were determined: 500–800 °C in the base metal and 800–1200 °C — in the weld metal.

3. The destruction nature and type, properties of welded joints of HTNA single-crystals, which are a composition of structural regions, are determined by the structural features of these regions, alongside the initial crystallographic orientation.

4. Failure of welded joints in 500–800 °C temperature range, considering the higher strength of the welds, which differ by a higher dispersity of the structure, takes place in the base metal. The fracture is mixed — brittle, quasibrittle, and ductile. At increase of testing temperature, the fraction of elements of brittle fracture (in the base metal) decreases with increase of the number of ductile fracture pits.

5. Failure of welded joints in the temperature range of 800–1200 °C, occurs in the weld, in connection with reduction of the strengthening effect of the finely-dispersed structure, dissolution of γ′-phase, activation of the diffusion processes and unblocking of dislocations. The fractures differ by multicellularity and are predominantly of a brittle nature with presence of local secondary microcracks and delaminations.

6. The type of fracture of welds, tested in the longitudinal direction in the temperature range of 500–800 °C, is characterized by prevalence of the ductile component with local areas of quasibrittle failure, at 800–1200 °C — the failure is mixed, with increase of volume fraction of the quasibrittle component with temperature rise, and presence of secondary cracks on the fracture surface. Unlike the welded joints in the transverse direction, the welds are characterized by a more homogeneous structure along their length.

7. Analysis of the properties and destruction features of welded joints, leads to the conclusion that development of the technology of fabrication of welded structures from single-crystal HTNA should be based on the need to preserve a homogeneous structure and properties of individual areas of the joint, along with taking into account the physical and technological conditions of preservation of the single-crystal structure.

## REFERENCES

1. Hurada, H. (2003) High temperature materials for gas turbines. The present and future. In: *Proc. of Int. Gas Turbine Congress-2003 (Tokyo, November 2–7)*.
2. Kablov, E.N., Petrushin, N.V., Svetlov, I.L., Demonis, I.M. (2007) Cast high-temperature nickel alloys for promising aviation gas-turbine engines. *Tekhnologiya Lyogkikh Splavov*, **2**, 6–16 [in Russian].
3. Kablov, E.N., Petrushin, N.V., Elyutin, E.S. (2011) Single-crystal high-temperature alloys for gas turbine engines. *Vestnik MGU, Ser. Mashinostroenie*, 38–52 [in Russian].
4. (2006) *Cast blades of gas turbine engines (alloys, technology, coatings)*. Ed. by E.N. Kablov. 2nd Ed. Moscow, Nauka [in Russian].

5. Kopelev, S.Z., Galkin, M.N., Kharin, A.A., Shevchenko, I.V. (1993) *Thermal and hydraulic characteristics of cooled gas turbine blades.* Moscow, Mashinostroenie [in Russian].
6. Fitzpatrick, G.A., Broughton, T. (1986) «Rolls-Royse Wide Chord Fan Blade». In: *Proc. of Int. Conf. on Titanium Products and Applications (San Francisco, California, USA, October 1986)*.
7. Yushchenko, K.A., Zadery, B.A., Gakh, I.S. et al. (2018) Prospects of development of welded single-crystal structures of high-temperature nickel alloys. *The Paton Welding J.*, **11–12**, 83–90.
8. Wang, N., Mokadem, S., Rappaz, M., Kurr, W. (2004) Solidification cracking of superalloy single- and bi-crystals. *Acta Materialia*, **52**, 3137–3182.
9. Park, J.W., Vitec, J.M., Bobu, S.S., David, S.A. (2004) Stray grain formation, thermomechanical stress and solidification cracking single crystal nickel base superalloy weds. *Sci. and Technol. of Welding and Joining*, 9(**6**), 472–482.
10. Anderson, T.D., DuPont, J.N. (2011) Stray grain formation and solidification cracking susceptibility of single crystal Ni-base superalloy CMSX-4. *Welding J.*, **2**, 27–31.
11. Yushchenko, K.A., Zadery, B.A., Zvyagintseva, A.V. et al. (2008) Sensitivity to cracking and structural changes in EBW of single crystals of heat-resistant nickel alloys. *The Paton Welding J.*, **2**, 6–13.
12. Yushchenko, K.A., Zadery, B.A., Gakh, I.S. et al. (2013) On nature of random orientation of grains in welds of single crystals of high-temperature nickel superalloys. *Metallofizika i Novejshie Tekhnologii*, 35(**10**), 1347–1357 [in Russian].
13. Yushchenko, K.A., Zadery, B.A., Gakh, I.S. et al. (2013) Influence of weld pool geometry on structure of metal of welds of high-temperature nickel alloy single crystals. *The Paton Welding J.*, **5**, 45–50.
14. Zvyagintseva, A.V. (2007) *Structural and phase transformations in high-temperature nickel alloys and their role in formation of cracks in welded joints*: Syn. of Thesis for Cand. of Tekh. Sci. Degree. Kyiv [in Russian].
15. (1961) *Radiography in physical materials science.* Ed. by Yu.A. Bagryansky. Moscow, Metallurgizdat [in Russian].
16. Krivoglaz, M.A. (1983) *Diffraction of X-ray beams and neutrons in abnormal crystals*. Kyiv, Naukova Dumka [in Russian].
17. Karasevskaya, O.P. (1999) Orientation X-ray experimental method of phase analysis. *Metallofizika i Novejshie Tekhnologii*, 21(**8**) [in Russian].
18. Panin, V.E., Egorushkin, V.E., Panin, A.V. (2006) Physical mesomechanics of deformable solid body as the multilevel system. I: Basic physics of multilevel approach. *Fizicheskaya Mezomekhanika*, 9(**3**), 9–22 [in Russian].
19. Rybin, V.V. (2002) Fundamentals of formation of mesostructures during developed plastic deformation. *Voprosy Materialovedeniya*, 29(**1**), 11–33 [in Russian].
20. Hall, E.O. (1951) The deformation and ageing of mild steel. III: Discussion of results. *Proc. Phys. Soc. B.*, **64**, 747–753.
21. Petch, N.J. (1953) The cleavage strength of polycrystals. *J. Iron Steel.*, **174**, 25–28.
22. Trefilov, V.I., Milman, Yu.V., Firstov, S.A. (1975) *Basic physics of strength of refractory metals*. Kyiv, Naukova Dumka [in Russian].
23. Jin-lai, Liu et al. (2011) Influence of temperature on tensile behavior and deformation mechanism of Re-containing single crystal superalloy. *Transact. Nonferrous Met. Soc. China*, **21**, 1518−1523.

**ORCID**
K.A. Yushchenko: 0000-0002-6276-7843,
I.S. Gakh: 0000-0001-8576-4234,
G.V. Zviagintseva: 0000-0002-6450-4887,
T.O. Aleksiienko: 0000-0001-8492-753X

**CONFLICT OF INTEREST**
The Authors declare no conflict of interest

**CORRESPONDING AUTHOR**
I.S. Gakh
E.O. Paton Electric Welding Institute of the NASU
11 Kazymyr Malevych Str., 03150, Kyiv, Ukraine
E-mail: gakh@paton.kiev.ua

**SUGGESTED CITATION**
K.A. Yushchenko, B.O. Zaderii, I.S. Gakh, G.V. Zviagintseva, T.O. Aleksiienko (2022) Destruction of welded joints of single-crystal high-temperature nickel alloys at tensile testing. *The Paton Welding J.*, **2**, 26–32.

**JOURNAL HOME PAGE**
https://pwj.com.ua/en

Received: 02.12.2021
Accepted: 31.03.2022